STM tunneling through a quantum wire with a side-attached impurity

T. Kwapiński, M. Krawiec, M. Jałochowski

*Institute of Physics and Nanotechnology Center, M. Curie-Skłodowska University,
Pl. M. Curie-Skłodowskiej 1, 20-031 Lublin, Poland*

Abstract

The STM tunneling through a quantum wire (QW) with a side-attached impurity (atom, island) is investigated using a tight-binding model and the nonequilibrium Keldysh Green function method. The impurity can be coupled to one or more QW atoms. The presence of the impurity strongly modifies the local density of states of the wire atoms, thus influences the STM tunneling through all the wire atoms. The transport properties of the impurity itself are also investigated mainly as a function of the wire length and the way it is coupled to the wire. It is shown that the properties of the impurity itself and the way it is coupled to the wire strongly influence the STM tunneling which is reflected in the density of states and differential conductance.

1 Introduction

The invention of scanning tunneling microscopy (STM) (1) was a milestone in experimental surface physics. Moreover, it became possible to tailor and analyze small nanostructures on various conducting surfaces (2; 3). Perhaps the most spectacular and pioneering examples are the quantum corral experiments, in which closed atomic structures were assembled with help of atomic manipulations (4). As the STM is a real space technique, and is very sensitive to the local atomic and electronic structures, it allows to study the properties of various, not necessarily periodic, structures with atomic resolution. Those include various surface reconstructions (3) and low dimensional structures, like single adatoms (2; 3), islands (5; 6) or one-dimensional monoatomic chains (7)-(10).

In particular, the one-dimensional structures are very interesting from a scientific point of view, as they exhibit extremely rich phenomena, very often different from those in two and three dimensions (11). However, in reality all the one-dimensional chains always stay in contact with their neighborhood (substrate, external electrodes, etc.), thus usually preventing the observations of the exotic physics. Moreover, very often they contain various imperfections, like impurities, dislocations or lacks of atoms. Such a situation likely takes place when those monoatomic chains are fabricated in self-assembly processes. The typical examples are all one-dimensional structures on vicinal Si surfaces (7; 8; 10).

The electron transport through a chain in two terminal geometry, in which the end atoms of the chain were coupled to external electrodes has been extensively studied, both experimentally and theoretically (see Ref. (12) for a review). A number of experiments has revealed many interesting phenomena, like conductance quantization in units of $G_0 = 2e^2/h$ (13), deviations from that (0.7 (G_0) anomaly) (14), spin-charge separation (Luttinger liquid) (15; 16), oscillations of the conductance as a function of the chain length (17; 18) or spontaneous spin polarization (14; 19). The problem of impurities or disorder in one-dimensional wires has also been studied both experimentally (20) and theoretically (21)-(26). The theoretical studies revealed that even a single impurity can lead to a dramatic modifications of the low energy physics. In particular, the conductance of a wire with interacting impurity shows a power law behavior with the scaling exponent depending on the strength of the impurity (24).

The problem of impurities (single atoms or clusters of atoms), but coupled sideways to a wire, has also been extensively studied recently (27)-(37). For a single impurity with a strong Coulomb interaction many authors predicted a suppression of the wire conductance due to the Fano interference between ballistic (wire) channel and the impurity channel (27)-(31). To be more precise, the Fano interference with the impurity reverses the gate voltage dependence of the conductance compared to the case when the impurity is embedded in a wire. The Fano effect in this case can have a 'classical' nature, if the interference comes from the impurity single particle channel, or a 'many-body' nature, when the resonant channel is formed by the Kondo effect at the impurity. The Fano effect in a wire with a side coupled quantum dot has been recently confirmed experimentally (32).

It is the purpose of the present paper to see what modifications of the transport properties of a chain introduce a side coupled impurity. Here, however, we shall study transport properties in different geometry, in which all the atoms in the chain as well as the impurity are coupled to one electrode and the second electrode is attached to one particular chain atom or the impurity via additional probing atom. This geometry simply corresponds to STM tunneling

2

through monoatomic chain with a side attached impurity, and can be related to previously mentioned STM study of self-assembled monoatomic chains on vicinal surfaces (7; 8; 10). To our knowledge, the problem in this geometry has not been studied experimentally so far, except the effects of impurities on the length distribution of atomic chains (38). Our system is described by tight binding model with no electron correlations, as we are not interested in many body effects like Kondo effect, metal-insulator transition, spin-charge separation, etc. So our model can be applied to the wires where the interaction energy is smaller than the kinetic energy associated with the hopping along the wire. For example, this could describe situation on various vicinal surfaces (like Si(335), Si(557), etc.) with monoatomic Au chains grown on them, where the correlation effects are negligible due to small carrier concentration (39). Moreover, the problem can be solved exactly in this case. In order to calculate the tunneling current we have adapted a non-equilibrium Keldysh Green's function technique. The organization of the rest of the paper is as follows. In Sec. 2 we introduce our model, and the results of the calculations and discussion are presented in Sec. 3. We end up with summary and conclusions.

2 The model

Our model system is shown schematically in Fig. 1 and is composed of a wire (w) with atomic energies ε_w and hopping integrals t_w between nearest neighbor atoms, impurity (a) with single energy level ε_a, which is side-coupled to the wire via hopping t_a. Both the wire and the impurity interact with the
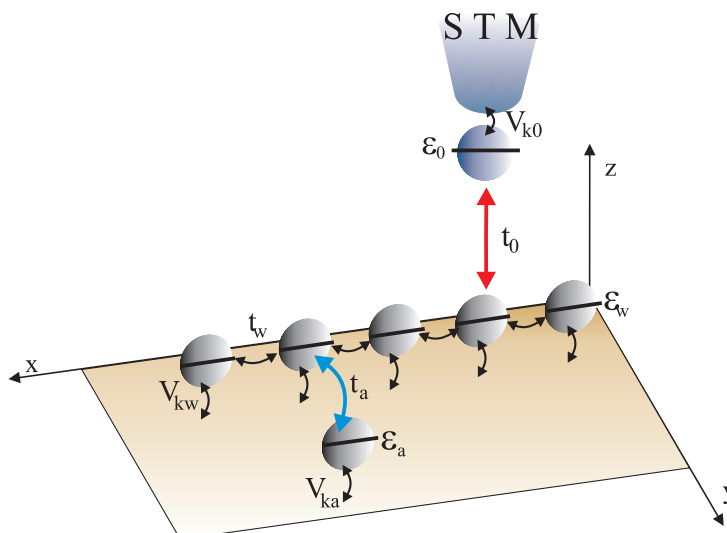

Fig. 1. Schematic view of the model STM system containing a chain with the side–coupled impurity.

surface (s) via $V_{\mathbf{k}w}$ and $V_{\mathbf{k}a}$, respectively. The surface is treated as a reservoir

for electrons with the wave vector $\mathbf{k}$, the spin σ and single particle energies $\epsilon_{s\mathbf{k}}$. Above the wire there is a STM tip (0) modeled by a single atom with the energy level ε_0 attached to another reservoir (t) (with electron energies $\epsilon_{t\mathbf{k}}$) via parameter $V_{\mathbf{k}0}$. Tunneling of the electrons between STM tip and one of the atoms in a wire is described by the parameter t_0. The whole system is described by the following model Hamiltonian

$$
\begin{aligned}
H = &\sum_{\lambda \in \{t,s\}\mathbf{k}\sigma} \epsilon_{\lambda\mathbf{k}} c^+_{\lambda\mathbf{k}\sigma} c_{\lambda\mathbf{k}\sigma} + \sum_\sigma \varepsilon_0 c^+_{0\sigma} c_{0\sigma} + \sum_{i\sigma} \varepsilon_w c^+_{i\sigma} c_{i\sigma} + \sum_\sigma \varepsilon_a c^+_{a\sigma} c_{a\sigma} \\
&+ \sum_\sigma (t_0 c^+_{0\sigma} c_{i\sigma} + H.c.) + \sum_{ij\sigma} (t_w c^+_{i\sigma} c_{j\sigma} + H.c.) + \sum_\sigma (t_a c^+_{a\sigma} c_{j\sigma} + H.c.) \\
&+ \sum_{\mathbf{k}\sigma} (V_{\mathbf{k}0} c^+_{t\mathbf{k}\sigma} c_{0\sigma} + H.c.) + \sum_{\mathbf{k}i\sigma} (V_{\mathbf{k}w} c^+_{s\mathbf{k}\sigma} c_{i\sigma} + H.c.) + \sum_{\mathbf{k}\sigma} (V_{\mathbf{k}a} c^+_{s\mathbf{k}\sigma} c_{a\sigma} + H.c.)
\end{aligned} \tag{1}
$$

where, as usually c^+_λ (c_λ) stands for the creation (annihilation) electron operator in the STM lead ($\lambda = t$), tip atom ($\lambda = 0$), wire ($\lambda = i$), impurity ($\lambda = a$) and the surface ($\lambda = s$).

In order to calculate the tunneling current from the STM electrode to the surface we follow the standard derivations (40; 41) and get

$$
I = \frac{e}{\hbar} \int \frac{d\omega}{2\pi} T(\omega)[f(\omega + eV/2) - f(\omega - eV/2)] , \tag{2}
$$

where $f(\omega)$ is the Fermi distribution function, $eV = \mu_t - \mu_s$ ($\mu_s = -\mu_t$) is the bias voltage, i.e. the difference between chemical potentials in the STM (μ_t) and the surface (μ_s) reservoirs, and the transmittance $T(\omega)$ is given in the form

$$
T(\omega) = \sum_\sigma \Gamma_t(\omega) \Gamma_s(\omega) | \sum_i G^r_{0i\sigma}(\omega) + G^r_{0a\sigma}(\omega)|^2 , \tag{3}
$$

with the coupling parameter $\Gamma_{t(s)}(\omega) = 2\pi \sum_{\mathbf{k}\in s(t)} |V_{\mathbf{k}0(w)}|^2 \delta(\omega - \epsilon_{t(s)\mathbf{k}})$ between the STM electrode (t) and the tip atom (0) and between the surface (s) and the wire (w). Note that, to get the above expression for the transmittance we have assumed the same values of the coupling of the wire and the impurity with the surface, i.e. $V_{\mathbf{k}w} = V_{\mathbf{k}i}$. $G^r_{0i\sigma}(\omega)$ ($G^r_{0a\sigma}(\omega)$) is the Fourier transform of the retarded Green's function (GF) $G^r_{0i(a)\sigma}(t) = i\theta \langle [c_{0\sigma}, c^+_{i(a)\sigma}]_+ \rangle$, i.e. the matrix element (connecting the tip atom 0 with ith atom in the chain or with the impurity a) of full GF, obtained from the solution of the equation

$$
(\omega \hat{1} - \hat{H}) \hat{G}^r(\omega) = \hat{1} \tag{4}
$$

The full GF $\hat{G}(\omega)$ is a $(N + 2) \times (N + 2)$ matrix (N atoms in a chain, the impurity and the tip atom), which is obtained by inverting the matrix $(\omega \hat{1} - \hat{H})$.

3 Results and discussion

Before the presentation of the numerical results, it is worthwhile to comment on choice of the model parameters used in the present work. In numerical calculations we have assumed equal and energy independent coupling parameters ($\Gamma_{t(s)}(\omega) = \Gamma_{t(s)}$), which reflects constant energy bands in both electrodes, and chosen $\Gamma_t = \Gamma_s = \Gamma$ as an energy unit. The other parameters have been chosen in order to satisfy the realistic situation in many experiments. The hopping integral within a wire is $t_w = 2$, $t_a = 1$, $t_0 = 0.1$, and $\varepsilon_w = 0$. For example, taking $\Gamma = 0.05$ eV, we get $t_w = 0.1$ eV, $t_a = 0.05$ eV, and $t_0 = 0.005$ eV. Such a value of the parameter t_0 together with the typical value of the work function $W = 5$ eV, gives a tip-surface distance $z = 6$ Å(10; 42), and the STM current stays in the range of a few nA. These are typical conditions in real STM experiments. Note that, with such a value of t_0, the modifications of the wire density of states due to the STM tip are negligible. In the following we will discuss the properties of wires containing even and odd number of atoms, as we expect different behavior for them, showing the results of the calculations for two representative examples, namely, for 4 and 5 atom wires. However the conclusions drawn from consideration of 4 (5) atom wire remain valid for any even (odd) N atom wire, provided the system is in ballistic regime. Moreover, we use the convention, in which the index i labels the wire atoms, while k indicates the position of the tip with respect to the wire atoms.

Let us first discuss the modifications of the wire density of states (DOS) due to the side-coupled impurity. The local DOS of ith atom in a wire is related to the corresponding diagonal element of the retarded GF, i.e. $\rho_i(\omega) = -\frac{1}{\pi}\sum_\sigma \mathsf{Im}G^r_{ii\sigma}(\omega)$. Similarly, for the impurity $\rho_a(\omega) = -\frac{1}{\pi}\sum_\sigma \mathsf{Im}G^r_{aa\sigma}(\omega)$.

Figure 2 shows a local DOS of a wire consisted of 4 (left panels) and 5 atoms (right panels) in various impurity-wire configurations, indicated in the insets to the panels. The top panels show the wire local densities of states in the case when there is no impurity attached, i.e. for clean wire. In this case, for N atom wire the local DOS on ith atom is the same as on $N + 1 - i$ atom ($\rho_i(\omega) = \rho_{N+1-i}(\omega)$), i.e. there is a symmetry with respect to the middle of the wire, thus the only non-equivalent $\rho_i(\omega)$ are plotted. For 4 atom wire the $\rho_i(\omega)$ has similar structure ($i = 1 = 4$ - thin solid line and $i = 2 = 3$ - thicker solid line) featuring small DOS at the Fermi energy $E_F = 0$ and resonances corresponding to the wire atomic energies $\varepsilon_w = 0$ split by the hopping $t_w = 2$. On the other hand, for 5 atom wire there are large DOS at the E_F, and the resonances are eventually split by t_w. Such a behavior is similar to the case of two terminal geometry in which the end wire atoms are connected to electrodes (17; 18; 34; 36; 43; 44; 45), i.e. a local minimum at the Fermi energy $E_F = 0$ for even number of atoms in a wire and local maximum at E_F for odd atom wire and can be explained in terms of bonding, antibonding and nonbonding
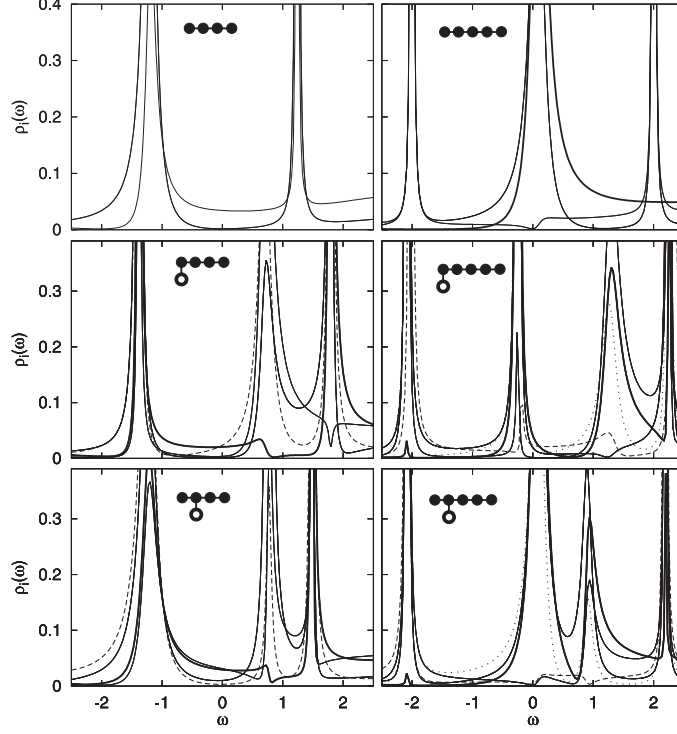
5

Fig. 2. The local DOS $\rho_i(\omega)$ in various wire-impurity configurations indicated in the insets. The left panels show $\rho_i(\omega)$ for 4 atom and the right ones for 5 atom wire, respectively. All the wire atomic energies as well as the tip apex energy are assumed to be zero ($\varepsilon_w = \varepsilon_0 = 0$), while the impurity energy level is $\varepsilon_a = 1$. Other parameters are described in the text. Thin solid lines correspond to the DOS on first wire atom ($i = 1$ from left), thicker solid line is for $i = 2$, thickest solid line is for $i = 3$, $i = 4$ is described by dashed, and $i = 5$ by dotted line.

states (43). In case of even atom wire there are always bonding ($\omega < E_F$) and antibonding ($\omega > E_F$) states. When N is odd, there is additional nonbonding state, which is situated at exactly the same position as the original atomic level ($\omega = \varepsilon_w$), thus giving large DOS at E_F, as $\varepsilon_w = E_F$ in our case. Interestingly, for the second (or second from the end) atom in an odd atom wire (thicker solid line in the top right panel), the situation is quite different, namely, the local DOS has very small value at the E_F. It turns out that this is a general tendency in odd atom wires, i.e. every second atom in an odd atom wire shows small DOS at the Fermi energy. This could be understood in the following way. Let us forget for a moment about the STM tip, as we mentioned previously, that the STM tip does not influence the wire DOS, and assume that the wire is coupled to the surface only. If we calculated number of non-equivalent electron paths starting and ending in the surface and passing through a given atom, it turns out that if the number of odd paths (passing through odd number of atoms) N_o is larger than the number of even paths (enclosing even number of atoms) N_e, then the local DOS has a resonance at E_F. Thus it behaves as in the case of odd atom wire in two terminal geometry with the end atoms coupled to the leads. For example, for the first atom in 5 atom wire (thin solid

line in the right top panel of Fig. 2) we get 5 non-equivalent odd paths and 4 even paths, thus $N_o > N_e$ and the resonance at the E_F is produced. Similarly, for the third atom, $N_o = 9$ and $N_e = 8$, and again $N_o > N_e$, thus we get the resonance at the Fermi energy (see thick solid line in the top left panel of Fig. 2). Opposite is also true, namely, if N_e is larger than N_o, the local DOS has similar behavior as in the case of even atom wire, featuring small $\rho_i(E_F)$. For example, $N_o = 7$ and $N_e = 8$ for the second atom in 5 atom wire (thicker solid line on the same picture as previously). This seems to be true for any number of atoms in a wire in the present geometry. Of course, this is only intuitive picture, well working in the present case, namely, when the system is in ballistic regime, so the phase coherence length is longer than the wire length. In general, in the presence of interactions (electron-electron, electron-phonon or scattering on magnetic impurities) the phase coherence length will be suppressed, and this simple picture can be no longer valid. In this case one has to calculate the contributions from different electron paths.

The middle and the bottom panels of Fig. 2 show the local densities of states $\rho_i(\omega)$ at different wire atoms in the case when the impurity with a single atomic level $\varepsilon_a = 1$ is attached to the first and second wire atom, respectively. The presence of the impurity introduces asymmetry in the DOS with respect to the middle of the wire, and the condition $\rho_i(\omega) = \rho_{N+1-i}(\omega)$ does not hold anymore, as a result $\rho_i(\omega)$ will be different on each wire atom. In both wires the main modification of the DOS features additional resonance and thus splitting by $\omega = t_a$ of the resonance around $\omega = 1$ ($\omega = 2$) in the case of 4 (5) atom wire. The low energy behavior of DOS is little affected, in particular for 4 atom wire. Accidentally, it may a little bit shift the zero energy resonance, leaving small DOS at E_F, as it is seen in the middle right panel of Fig. 2. This will be also reflected in the linear conductance, as we will see later.

In two terminal geometry, when the end wire atoms are connected to two different leads, the useful quantity is the total density of states, as in this case the conductance of the system is correlated with it (34). On the other hand, in the STM geometry we do not expect that the behavior of the conductance will be governed by this quantity. To see this, we plotted the total (wire plus impurity) density of states $\rho(\omega)$ of a chain consisted of 4 atoms (left panel) and 5 atoms (right panel of Fig. 3). The total DOS is defined as a $\rho(\omega) = \sum_i \rho_i(\omega)/N$ for the wire with no impurity attached, and as a $\rho(\omega) = (\sum_i \rho_i(\omega) + \rho_a(\omega))/(N+1)$ in the case when the impurity is present. We have distinguished two cases, namely, when the impurity has the same value of the atomic energy $\varepsilon_a = 0$ as for the wire atoms, and when it has different energy $\varepsilon_a = 1$. The former case would correspond to the situation when the wire atoms and the impurity are composed of the same material, while in the later one, the impurity is a different atom.

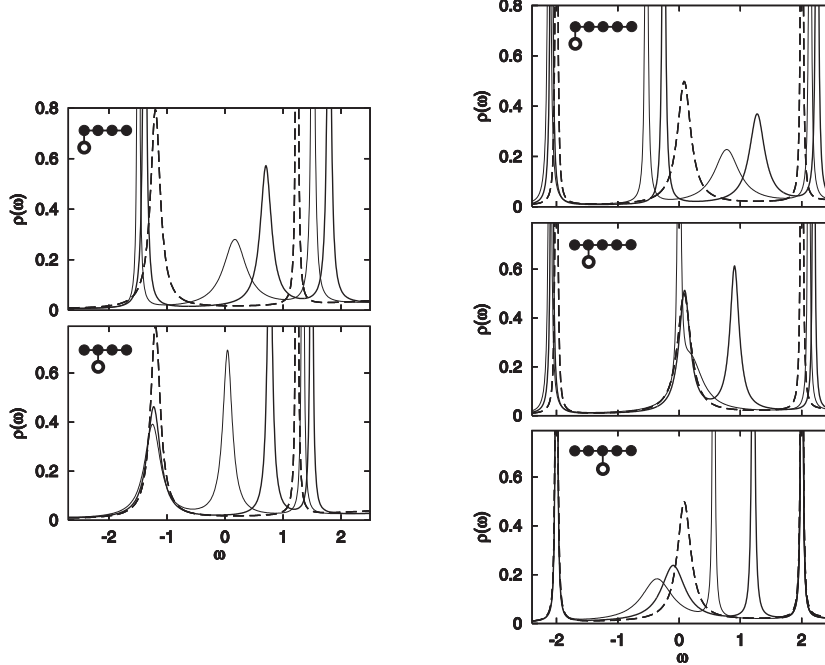First of all, if there is no impurity (dashed lines) the total DOS shows simi-

Fig. 3. Total density of states of a wire consisted of 4 atoms (left panels) and 5 atoms (right panels) with side-coupled impurity. All the wire atomic energies ε_w are equal to zero, while the impurity energy level $\varepsilon_a = 1$ (thick solid lines) and $\varepsilon_a = 0$ (thin solid lines). The dashed lines represent the wire total DOS in the lack of the impurity. The insets show schematic configurations of the wire-impurity, i.e. the positions of the impurity with respect to the wire atoms.

lar behavior as in the case of the end wire atoms coupled to the leads only. However one can notice different heights of particular resonances. This reflects an effect, known from the studies of two impurities on a surface, and associated with different (even-odd) symmetries of electron states in resulting system (46). When the impurity is introduced to the system, the total DOS is strongly modified due to the parameter t_a, which is responsible for the hoping between those subsystems. In this case t_a is only two times smaller than the wire hoping t_w, thus one should expect modifications of the wire DOS. The impurity usually introduces additional resonance to the total DOS. In both cases the position of the resonance is around its atomic energy (compare thin and thick solid lines in in the left panels of Fig. 3), and slightly modifies the resonances coming from the wire atoms. This behavior only slightly depends on which wire atom is in close connection with the impurity.

Let us now turn to the transmittance $T(\omega)$, defined by Eq. (3). Figure 4 shows the transmittance of the system in various STM tip-wire-impurity configurations for 4 atom (left panels) and 5 atom wire (right panels). While the transmittance depends on the STM tip position now, it is possible to identify the impurity induced contribution to $T(\omega)$. The impurity introduces additional resonance to $T(\omega)$ around its atomic energy, i.e. at $\omega = \varepsilon_a$ (compare the left panels of Fig. 4). In both cases, i.e. for 4 and 5 atom wires, the transmittance
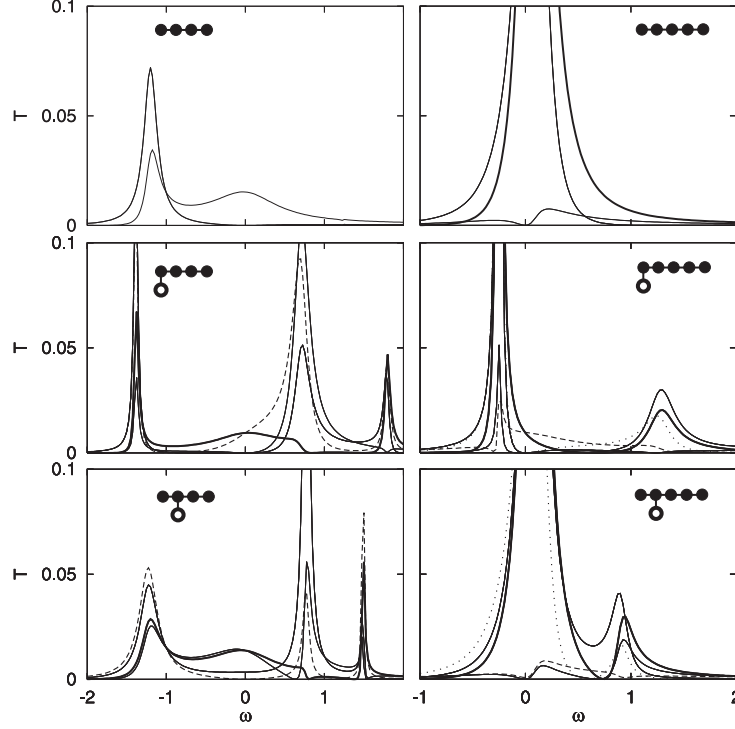
8

Fig. 4. Transmittance $T(\omega)$ of the system in various wire-impurity configurations indicated in the insets and various positions of the STM tip. The left panels show $T(\omega)$ for 4 atom and right panels for 5 atom wire, respectively. The impurity energy level is now $\varepsilon_a = 1$. Thin solid line corresponds to the STM tip above first wire atom ($k = 1$ from left), thicker solid line is for $k = 2$, thickest solid line is for $k = 3$, $k = 4$ is described by dashed, and $k = 5$ by dotted line.

is correlated with the local density of states, and the presence of the impurity leads to similar modifications, especially for $\omega = 0$ (compare Fig. 2), although the transmittance is now more asymmetrical. This is in contradiction with the transport along the wire, as in that case the transmittance depends on the total DOS. Here it depends on the local DOS. Explanation is simple and intuitive. In the transport along the wire, all the local DOS equally contribute to the transmittance (34). In the present case, the transport takes place mainly through the wire atom, just below the STM tip, thus $T(\omega)$ depends mainly on the local DOS of a particular atom.

The presence of the impurity usually leads to higher values of $T(\omega)$ for the resonances of the wire origin. Such a behavior is in contradiction with the behavior of $T(\omega)$ when the transport takes place along the wire. In the former geometry this leads to the reduction of the conductance (27)-(31). Here however, the situation is different, as the impurity is also connected to the same lead as the wire is, thus the impurity provides additional tunneling channel. Nevertheless, the zero energy transmittance is influenced by the impurity, similarly as the local DOS (compare Fig. 2).

9

At this point we would like to comment on the Fano effect, as there are many channels for electron tunneling from STM tip to the surface. Even the tip is 'coupled' to a single wire atom, the electron can leave the wire entering the surface electrode through different wire atoms. This is particularly well visible for STM tip placed above second atom in odd atom wire even without impurity attached (thicker solid line in top right panel of Fig. 4). In this case odd number atoms in the wire have large density of states at the Fermi energy, while even atoms have small DOS at E_F (see Fig. 2). When the STM tip is placed above first (thin solid line) or third (thickest solid line) an electron can tunnel through undelaying atom directly to the surface because neighboring atoms have small DOS at E_F. The Fano effect is negligible in this case. On the countrary, when the tip is placed above second atom, which has small DOS at E_F (thicker solid line), the electron has three tunneling channels to the surface, due to large values of DOS at neighboring atoms. It can directly tunnel to the surface or go through first or third wire atom. In this case the Fano effect is enhanced and is visible as a dip at the Fermi energy. The presense of impurity slightly modifies the above picture, usually enhancing the Fano effect when the tip is above the wire atom with attached impurity. Compare thin solid line in midle right panel of Fig. 4 and thicker solid line in the bottom right panel. We do not observe Fano effect for even atom wire because DOS at E_F is always small (see Fig. 2).

Similar effects are reflected in differential conductance $G = dI/d(eV)$, shown in Fig. 5. Again, the presence of the impurity leads to a increase of G around $eV = 2\varepsilon_a$ (note that $eV = \mu_s - \mu_t$ and $\mu_s = -\mu_t$), thus can help us in studying of the properties of impurities attached to wire in real STM experiments. It also modifies the structures coming from the wire atoms, also leading to larger values of G. Note however, that the values of G are much smaller ($0.12\ e^2/h$ for 4 atom and 0.55 for 5 atom wire) than the conductance unit, i.e. e^2/h per tunneling channel. This is due to small value of the STM tunneling parameter t_0. For $t_0 = 1$, the conductance reaches the unitary limit, i.e. $2e^2/h$ in our case (two spin channels). On the other hand, the linear conductance, i.e. $G(eV = 0)$ strictly follows the local density of states, similarly as the zero energy transmittance (compare Fig. 5 and Figs. 2 and 4). In a special case when the impurity is coupled to the first atom in 5 atom wire, the zero bias maximum is split and the linear transport is strongly reduced for any wire atom (compare the middle right panel of Fig. 2).

So far we have discussed the various configurations, in which impurity was coupled to a single atom wire. This would correspond to a situation in which the impurity is placed close to one particular wire atom. Now, the question arises what will happen if the impurity is side-coupled to two wire atoms, i.e. is placed aside between two wire atoms. Figure 6 shows the conductance changes due to different couplings of the impurity to one atom (top panel) and two atoms in a wire (bottom panel). Both panels show the conductance maps
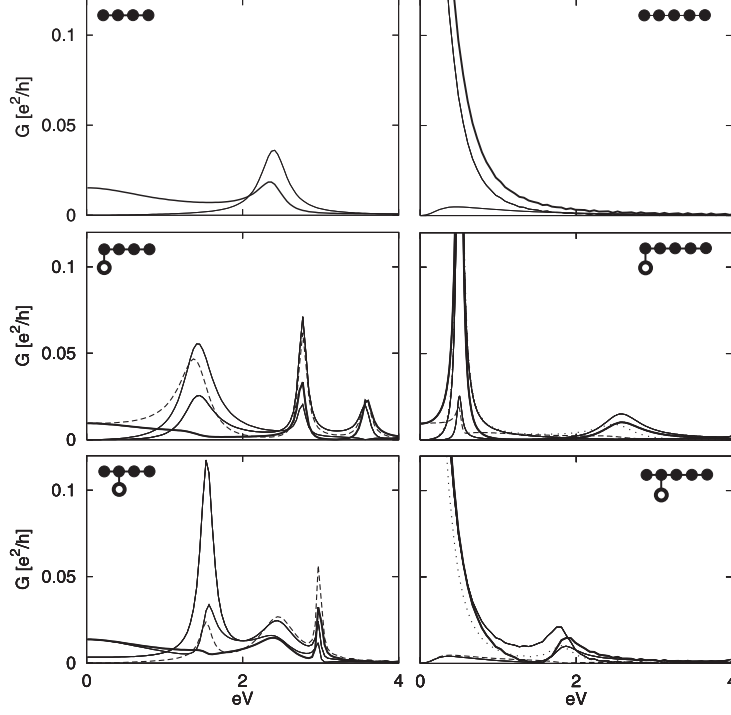
Fig. 5. Corresponding differential conductance vs. bias voltage of the system in the same impurity-wire configurations, as in Fig. 4. The parameters and the meaning of the curves are the same as those in Fig. 4.

vs. bias voltage eV and corresponding couplings t_{a2} (t_{a3}) (see the insets to the figure). In first configuration (top panel) the impurity is coupled to one wire atom, and the differential conductance has a maximum in the plane (eV, t_{a2}). The position of the maximum changes linearly with eV and t_{a2}. On the other hand, in second configuration, when the strength of the impurity coupling changes (bottom panel), i.e. for various positions of the impurity between second and third wire atom, we see that the largest values of G are obtained when the impurity is close to the second atom ($t_{a3} \approx 0$, $t_{a2} \approx 2$) and slightly smaller close to the third wire atom ($t_{a2} \approx 0$, $t_{a3} \approx 2$). For intermediate values of t_{a2} (t_{a3}) the conductance is strongly reduced, in particular, when $t_{a2} = t_{a3}$. This is due to the Fano effect, which is further enhanced in this case, and leads to similar reduction of G in the case of two terminal geometry with the end wire atoms coupled to the leads (27)-(31). The fact, that the maximal values of the differential conductance show asymmetry with respect to $t_{a2} = t_{a3}$ point, i.e. they are different for the impurity near the second wire atom and near the third wire atom steams from the fact that STM tip is placed above the second wire atom.

Finally we would like to comment on the Coulomb interactions, as the present model completely neglects them. We expect qualitative modifications of the results (like even-odd oscillations of density of states), especially at low temperatures where the Coulomb blockade and the Kondo effect take place. The
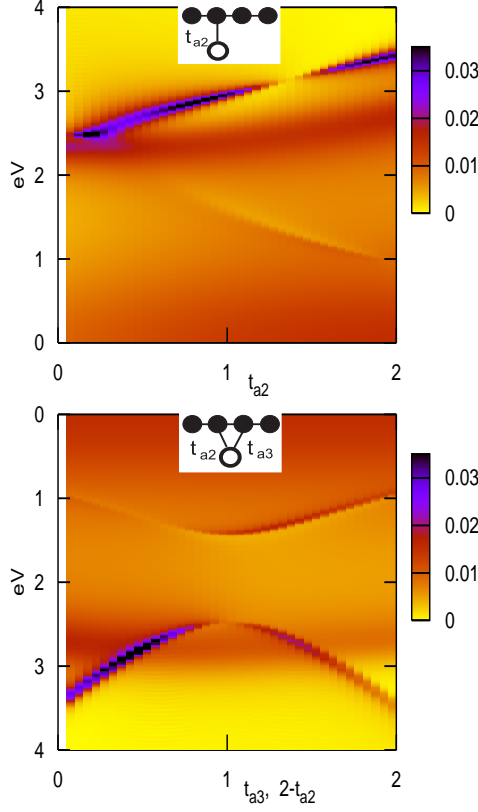
11

Fig. 6. Differential conductance vs eV and t_a. Top panel represents the situation when the impurity is coupled to the second wire atom via the parameter t_{a2}. The bottom panel shows G in the case when the impurity is coupled to the second and the third wire atom via t_{a2} and t_{a3} ($t_{a3} = 2 - t_{a2}$), respectively.

picture can change drastically (6). The tunneling can be enhanced when the wire energy levels are placed below the Fermi energy and the wire is strongly coupled to the surface (Kondo effect) or suppressed when it is weakly coupled, leading to the Coulomb blockade. The presense of additional tunneling channel (due to the Kondo effect) can also enhance the Fano effect. On the other hand, we do not expect qualitative modifications in the mixed valence and the empty regimes, i.e. when the wire energy levels are above the Fermi energy. The present model can be succesfully applied to study monoatomic (Au, Ag, Pb) chains grown on various vicinal surfaces (7)-(10).

4   Conclusions

In conclusion we have studied STM tunneling through a quantum wire with a side-coupled impurity in various coupling configurations, i.e. the impurity was coupled to various atoms in a wire, and moreover, it was also connected to more than single wire atom. We have found that the impurity strongly modifies the

transport properties. In particular it always produces a resonance around its atomic energy, which can be seen in differential conductance vs. bias voltage. Moreover, we have also shown that if the impurity is side-coupled to two wire atoms with equal strength, it leads to the suppression of the conductance, which is a hallmark of the Fano effect in such a system. Those studies could be potentially useful in STM studying of the impurity induced modifications of the wire properties.

Acknowledgements

Appendix

In this appendix we give analytical solutions/relations for the local density of states (LDOS) of a wire disturbed by an adatom. LDOS is connected with the retarded Green's function by the following relation

$$LDOS_i(\omega) = \frac{-1}{\pi} Im G_{ii}^r(E) \tag{5}$$

where $G^r(E)$ can be obtained from the equation of motion for Green functions. Using Eq. 2 one can write

$$\hat{G}_{ii}^r(\omega) = (\omega \hat{1} - \hat{H})^{-1} = \hat{Z}_{ii}^{-1} = \frac{\text{cof}\,\hat{Z}_{ii}}{\det \hat{Z}} \tag{6}$$

where $\text{cof}\,\hat{Z}_i$ is the algebraic complement of the matrix $\hat{Z}$ (cofactor). In our calculations we assume the same coupling strengths between atoms, t_w, and the same single particle energies ε_w for all atoms in the wire. It is worth noting that the STM is weakly coupled with the wire and thus it does not affect the wire density of states (in Hamiltonian Eq. (1) we put $t_0 = 0$).

First we consider the case of a linear wire without an adatom i.e. $t_a = 0$. In this case LDOS can be obtained from the relation $LDOS_{ii}(\omega) = -Im\text{cof}\,\hat{A}_{ii}^N/\pi \det \hat{A}^N$ where

$$\hat{A}^N = \hat{A}_{k_1 k_2}^N = (\varepsilon - \varepsilon_w)\delta_{k_1,k_2} - t_w(\delta_{k_1,k_2+1} + \delta_{k_1+1,k_2}) - \Sigma_S \tag{7}$$

13

and $\Sigma_S = -i\Gamma/2$, $k_1, k_2 = 1, ..., N$. To obtain LDOS one needs to know the determinant of $\hat{A}^N$ which can be expressed as follows

$$\det \hat{A}^N = \det \hat{A}_0^N - \Sigma_S \sum_{k=1}^{N} \det \hat{A}_0^{N-k} \sum_{l=1}^{k-1} (-t_w)^{k-l} \det \hat{A}_0^{l-1}$$

$$-\Sigma_S \sum_{k=1}^{N} \det \hat{A}_0^{k-1} \sum_{l=k}^{N} (-t_w)^{l-k} \det \hat{A}_0^{N-l} \tag{8}$$

The matrix $\hat{A}_0^N$ corresponds to an isolated wire (non-coupled with the surface) and is a tridiagonal one, $\hat{A}_0^N = \hat{A}_{k_1 k_2}^N + \Sigma_S$, and can be expressed analytically in terms of Chebyshev polynomials of the second kind (34).

The LDOS for a wire coupled with an adatom can be obtained from the relation $LDOS_{ii}(\omega) = -Im \mathtt{cof} \hat{B}_{ii}^{N+1}/\pi \det \hat{B}^{N+1}$ where

$$\hat{B} = \begin{pmatrix} \hat{A}^N & \hat{X}^T \\ \hat{X} & \varepsilon - \varepsilon_a \end{pmatrix} \tag{9}$$

and $\hat{X}$ is a vector describing the couplings adatom-QW and adatom-surface, $\hat{X} = -(\Sigma_S, ..., t_a + \Sigma_S, ..., \Sigma_S)$ (j-th atom of a wire is connected with the adatom. After some algebra the determinant of the above matrix can be written in the form

$$\det \hat{B}^{N+1} = (\omega - \varepsilon_a) \det \hat{A}^N - \Sigma_S \det \hat{A}_0^N + t_a \mathtt{cof} \hat{A}_{jj}^{N-1} +$$

$$2t_a \sum_{k=1}^{N} (-1)^{k+j} (t_w)^{|j-k|} \det \hat{A}_0^{\min(k,j)-1} \det \hat{A}_0^{N-\max(k,j)} \tag{10}$$

Similar equation one can write for $\mathtt{cof} \hat{A}^N$ and $\mathtt{cof} \hat{B}^{N+1}$ which also can be expressed in terms of $\det \hat{A}_0$ but have more complicated structure. For the case $\Sigma_S = 0$ (there is no surface under the wire or the coupling wire-surface is very weak) one can easily find

$$\det \hat{B}^{N+1} = (\omega - \varepsilon_a) \det \hat{A}_0^N - t_a^2 \det \hat{A}_0^{j-1} \det \hat{A}_0^{N-j} \tag{11}$$

$$\mathtt{cof} \hat{B}_{ii}^{N+1} = (\omega - \varepsilon_a) \det \hat{A}_0^{j-1} \det \hat{A}_0^{N-j} + t_a^2 \det \hat{A}_0^{\min(i,j)} \det \hat{A}_0^{|i-j|-1} \det \hat{A}_0^{N-\max(i,j)} \tag{12}$$

and the LDOS can be obtained fully analytically. It is worth noting that the determinants $\det \hat{A}$, $\det \hat{B}$ and $\det \mathtt{cof} \hat{B}$ are obtained for arbitrary j (connection adatom-QW atom) and N (even or odd). The minima of $|\det \hat{B}|^2$ determine high value of LDOS and the conductance through the system.

References

[1] G. Binnig, H. Rohrer, Ch. Gerber, E. Weibel, Appl. Phys. Lett. **40**, 178 (1982); Phys. Rev. Lett. **49**, 57 (1982).

[2] G. A. D. Briggs, A. J. Fisher, Surf. Sci. Rep. **33**, 1 (1999).

[3] W. A. Hofer, A. S. Foster, A. L. Shluger, Rev. Mod. Phys. **75**, 1287 (2003).

[4] M. F. Crommie, C. P. Lutz, D. M. Eigler, Science **262**, 218 (1993); E. J. Heller, M. F. Crommie, C. P. Lutz, D. M. Eigler, Nature **369**, 464 (1994).

[5] M. Jałochowski, Prog. Surf. Sci. **74**, 97 (2003).

[6] M. Krawiec, M. Jałochowski, M. Kisiel, Surf. Sci. **600**, 1641 (2006).

[7] F. J. Himpsel, K. N. Altmann, R. Bennewitz, J. N. Crain, A. Kirakosian, J. -L. Lin, J. L. McChesney, J. Phys.: Condens. Matter **13**, 11097 (2001).

[8] J. N. Crain, J. L. McChesney, Fan Zheng, M. C. Gallagher, P. C. Snijders, M. Bissen, C. Gundelach, S. C. Erwin, F. J. Himpsel, Phys. Rev. **B69**, 125401 (2004).

[9] M. Jałochowski, M. Stróżak, R. Zdyb, Appl. Surf. Sci. **211**, 209 (2003).

[10] M. Krawiec, T. Kwapiński, M. Jałochowski, phys. stat. sol. **(b)242**, 332 (2005); Phys. Rev. **B73**, 075415 (2006).

[11] J. M. Luttinger, J. Math. Phys. **4** 1154 (1963); F. D. M. Haldane, J. Phys. C: Solid State Phys. **14** 2585 (1981); J. Voit, Rep. Prog. Phys. **58**, 977 (1995).

[12] N. Agrait, A. Levy Yeyati, J. M. van Ruitebeek, Phys. Rep. **377**, 81 (2003).

[13] B. J. van Wees, H. van Houten, C. W. J. Beenakker, J. G. Williamson, L. P. Kouwenhoven, D. van der Marel, C. T. Foxon, Phys. Rev. Lett. **60**, 848 (1988).

[14] K. J. Thomas, J. T. Nicholls, M. Y. Simmons, M. Pepper, D. R. Mace, D. A. Ritchie, Phys. Rev. Lett. **77**, 135 (1996).

[15] O. M. Auslaender, A. Yacoby, R. de Picciotto, K. W. Baldwin, L. N. Pfeiffer, K. W. West, Phys. Rev. Lett. **84**, 1764 (2000).

[16] O. M. Auslaender, H. Steinberg, A. Yacoby, Y. Tserkovnyak, B. I. Halperin, K. W. Baldwin, L. N. Pfeiffer, K. W. West, Science **308**, 88 (2005).

[17] C. J. Muller, J. M. van Ruitenbeek, L. J. de Jongh, Phys. Rev. Lett. **69**, 140 (1992).

[18] R. H. M. Smit, C. Untiedt, G. Rubio-Bollinger, R. C. Segers, J. M. van Ruitenbeek, Phys. Rev. Lett. **91**, 076805 (2003).

[19] B. E. Kane, G. R. Facer, A. S. Dzurak, N. E. Lumpkin, R. G. Clark, L. N. Pfeiffer, K. W. West, Appl. Phys. Lett. **72**, 3506 (1998).

[20] W. H. A. Thijssen, D. Marjenburgh, R. H. Bremmer, J. M. van Ruitenbeek, Phys. Rev. Lett. **96**, 026806 (2006).

[21] A. Luther, I. Peschel, Phys. Rev. **B9**, 2911 (1974).

[22] T. Giamarchi, H. J. Schulz, Phys. Rev. **B37**, 325 (1988).

[23] F. Dolcini, H. Grabert, I. Safi, B. Trauzettel, Phys. Rev. Lett. **91**, 266402 (2003); F. Dolcini, B. Trauzettel, I. Safi, H. Grabert, Phys. Rev. **B71**, 165309 (2005).

[24] T. Enss, V. Meden, S. Andergassen, X. Barnabé-Thériault, W. Metzner, K. Schönhammer, Phys. Rev. **B71**, 155401 (2005).

[25] A. Agarwal, D. Sen, Phys. Rev. **B73**, 045332 (2006).

[26] M. M. Fogler, S. V. Malinin, T. Nattermann, cond-mat/0602008.

[27] K. Kang, S. Y. Cho, J.-J.Kim, S.-C. Shin, Phys. Rev. **B63**, 113304 (2001).

[28] M. E. Torio, K. Hallberg, A. H. Ceccatto, C. R. Proetto, Phys. Rev. **B65**, 085302 (2002); M. E. Torio, K. Hallberg, S. Flach, A. E. Miroshnichenko, M. Titov, Eur. Phys. J. **B37**, 399 (2004); M. E. Torio, K. Hallberg, C. R. Proetto, cond-mat/0404146.

[29] A. A. Aligia, C. R. Proetto, Phys. Rev. **B65**, 165305 (2002).

[30] R. Franco, M. S. Figueira, E. Anda, Phys. Rev. **B67**, 155301 (2003).

[31] P. Stefański, Solid State Commun. **128**, 29 (2003).

[32] K. Kobayashi, H. Aikawa, A. Sano, S. Katsumoto, Y. Iye, Phys. Rev. **B70**, 035319 (2004).

[33] T. Kwapiński, Vacuum **74**, 201 (2004).

[34] T. Kwapiński, J. Phys.: Condens. Matter **17**, 5849 (2005); *ibid* **18**, 7313 (2006).

[35] V. Puthier, C. Girarded, Surf. Sci. **511**, 203 (2002).

[36] P. A. Orellana, F. Domingues-Adame, I. Gomez, M. L. Ladron de Guevara, Phys. Rev. **B67**, 085321 (2003).

[37] K. S. Thygesen, M. V. Bollinger, K. W. Jacobsen, Phys. Rev. **B67**, 115404 (2003).

[38] J. N. Crain, M. D. Stiles, J. A. Stroscio, D. T. Pierce, Phys. Rev. Lett. **96**, 156801 (2006).

[39] J. N. Crain, A. Kirakosian, K. N. Altmann, C. Bromberger, S. C. Erwin, J. L. McChesney, J. -L. Lin, F. J. Himpsel, Phys. Rev. Lett. **90**, 176805 (2003).

[40] H. Haug, A. P. Jauho, *Quantum Kinetics in Transport and Optics of Semiconductors* (Springer, Berlin, 1996).

[41] M. Krawiec, K. I. Wysokiński, Solid State Commun. **115**, 141 (2000); Semicond. Sci. Technol. **17**, 103 (2004).

[42] Y. Calev, H. Cohen, G. Cunibereti, A. Nitzan, D. Porath, Isr. J. Chem. **44**, 133 (2004).

[43] F. Liu, S. N. Khanna, P. Jena, Phys. Rev. **B42**, 976 (1990).

[44] Z. Y. Zeng, F. Claro, Phys. Rev. **B65**, 193405 (2002).

[45] M. Krawiec, T. Kwapiński, Surf. Sci. **600**, 1697 (2006).

[46] D. M. Newns, N. Read, Adv. Phys. **36**, 799 (1987).